

Article

The Impact of Viscous Dissipation on the Thin Film Unsteady Flow of GO-EG/GO-W Nanofluids

Ali Rehman ^{1,*}, Zabidin Salleh ^{1,*}, Taza Gul ² and Zafar Zaheer ³

¹ School of Informatics and Applied Mathematics, Universiti Malaysia Terengganu, Kuala Nerus 21030, Terengganu, Malaysia

² Department of Mathematics, City University of Science and Information Technology, Peshawar 25000, Pakistan

³ Institute of Management Sciences, Peshawar 25000, Pakistan

* Correspondence: zabidin@umt.edu.my

Received: 17 May 2019; Accepted: 17 July 2019; Published: 20 July 2019



Abstract: The unsteady flow of nanoliquid film over a flexible surface has been inspected. Water and ethylene glycol are used as the base liquids for the graphene oxide platelets. The comparison of two sorts of nanoliquids has been used for heat transfer enhancement applications. The thickness of the nanoliquid film is kept as a variable. The governing equations for the flow problem have been altered into the set of nonlinear differential equations. The BVP 2.0 package has been used for the solution of the problem. The sum of the square residual error has been calculated up to the 10th order approximations. It has been observed that the graphene oxide ethylene glycol based nanofluid (GO-EG) is more efficient for heat transfer enhancement as compared to the graphene oxide water based nanofluid (GO-W). The impact of the physical parameters has been plotted and discussed.

Keywords: GO-W/GO-EG nanofluids; thin film; unsteady stretching sheet; viscous dissipation; BVP 2.0 package

1. Introduction

Nanofluid is defined as the homogeneous mixture of Nano size particles and base fluid. The thermal conductivity of the standard base fluids, such as oil, ethylene, and water is very small. To improve the thermal efficiency of the base fluid for the enhancement of the heat transfer rate, researchers have immersed the nanoparticles into the base fluid. Choi [1] is the pioneer to introduce the name of the Nano particle. In the field of technology covering chemical production, power stations, and microelectronics, there is a need to recommend new types of fluids that are more active with respect to the heat exchange process. For this reason, Nanofluids are composed to guarantee operative thermal conductivity developments and to achieve the uprising masses of cooling/heating and other materials. Nanofluid is a spreading consisting of nanometer-sized particles (1–100 nm) in size, called nanoparticles. The proper applications of the nanoparticles and the dispersion of the nanoparticles in the base fluid can be seen in the work of Choi et al. [2]. Haq et al. [3] inspected the nanofluid thermal efficiency, over a trapezoidal cavity by using the finite element method. They observed the heated domain partially by increasing the temperature. Soomro et al. [4] analyzed nanoparticle movement over a stretching plate by using passive methods.

Yu et al. [5] found the thermal conductivity and viscosity to discuss the thermal carrying properties of ethylene glycol-based nanofluid. Xie and Chen [6] investigated that idea that the thermal conductivity of the base fluid is much less than that of the graphene oxide nanosheet. To fulfill this space, Xiao et al. [7] tried to model an analytical expression for the thermal conductivity of the nanofluid by using the result of heat convection. Buongiorno [8] studied a complete analysis of the nanofluid. Khan and

Pop [9] investigated the motion of nanofluid by using stretching plate. Shah et al. [10] studied the effects of hall current on steady three-dimensional non-Newtonian nanofluid in a rotating frame with Brownian motion and thermophoresis properties. The thermal conductivity and stability of carbon based nanofluids is very high, visual properties of dynamic surface area, environmental and mechanical stability of carbon-based fluid is satisfactory, due to the electronic hybridization of sp , sp^2 , sp^3 . Carbon is an arresting component, graphene is defined as the single coated 2D sheets of graphite. Graphene is mostly used as a nanofluid as the organized potential wall of the solubility is very poor. Thus, we used graphene in the form of graphene oxide (GO), as it changes as a result and forms indisputable dispersion in water due to its high oxidize structure. GO is solvable in oils, the dynamic research area of GO is practically in the rotating disk model of nanofluids. Graphene is a single layer of carbon atom in a hexagonal lattice. The researchers take more interest in graphene oxide as compared to graphene. Graphene oxide (GO) is a two-dimensional material, and it is the oxidized form of graphene with O functional groups. Graphene oxide (GO) was first synthesized in 1859 by Sir Second Baronet Benjamin Colline Brodie via oxidation of bulk graphite with potassium chlorate and nitric acid by chemical method. The natural structure has been studied by Lerf and Klinowsky, at present the most well-known method to synthesize graphene oxide (GO) is the modified hummers method.

The most important application of GO is for industrial machinery and many engineering apparatuses, for example, turbine systems, centrifugal pump rotating blades, turbo machinery hard disk jet motors, and computer storage systems. The central purpose of GO nanofluid flow is the stability of centrifugal forces by engaging the circular pressure gradient. Heat transfer is one of the important properties in chemical processes, which is affected by the base fluid, such as water and mineral oil. The heat transfer properties of mineral oil is lower than water, thus a different method must be used to increase heat transfer, for example: reduced heat transfer or time heat exchangers size can be minimized. Ethylene Glycol (EG) can be used as a cooling fluid and anti-freezing agent to improve thermal properties because the thermal conductivity of the metallic and nonmetallic and carbon structures are much higher than the base fluids.

Balandin et al. [11] studied the single-layer graphene in various base solvents to improve the thermal efficiency of the base fluids. The stable diffusion of the graphene oxide in the ethylene glycol for the enhancement of heat transfer was first analyzed by Wei et al. [12].

Gul et al. [13] investigated the experimental study to examine the stable dispersion of the graphene nanoparticle and to look at the GO- H_2O nanofluid by using two rotating discs. Gul et al. [14] examined the water and ethylene glycol-based graphene oxide nanofluid flow under the influence of Marangoni convection. They analyzed the impact of the physical constraints and compared the effect of the embedded parameters using the GO-W and GO-EG nanofluids. The thin film is a thin layer of the fluid having finite domain. Qasim et al. [15] studied heat and mass transfer in nanofluid thin film over an unsteady stretching sheet using Buongiorno's model.

Ali and Gul [16] examined the thin film nanofluid flow with variable thickness over a stretching surface. Gul et al. [17] studied the two types of alumina oxide nanofluid with variable thickness of the thin film over an extending surface of a cylinder. Considering thin film, Aziz et al. [18] investigated the thin film flow and heat transfer on an unsteady stretching sheet with internal heating. Pour et al. [19] discussed numerical investigation of forced laminar convection flow of nanofluids over a backward facing step under bleeding condition. Abu-Nada et al. [20] investigated numerical prediction of entropy generation in separated flow. Abu-Nada et al. [21] investigated the application of nanofluids for heat transfer enhancement of separated flows encountered in a backward facing step.

In this paper, the thin film unsteady flow of GO-EG and GO-W nanofluid in the presence of viscous dissipation have been examined. The comparison of the GO-EG and GO-W have been analyzed under the influence of the physical parameters. The problem has been solved through the optimal homotopy analysis method (OHAM) as described by Liao et al. [22]. This method is frequently used for the solution of nonlinear problems and shows that this method is quickly convergent to the approximate solution. This method is further modified by the Liao [23] for the fast convergence of the nonlinear

problem by introducing the BVP 2.0 package. The researchers [24–30] used this method for the various nonlinear problems occurring in the field of science and engineering.

2. Mathematical Formulation

Consider the unsteady flow of graphene oxide water and ethylene glycol (GO-W/GO-EG) based nanofluids over a flexible sheet. $U_w = \frac{bx}{1-\gamma t}$ is the unsteady flexible velocity of the sheet in the x -direction, such that b, γ are the positive constants and t is the term used for the time. The temperature distribution $T_w(x, t) = T_0 - T_r \left(\frac{bx^2}{2v}\right) (1-\gamma t)^{-\frac{3}{2}}$ on the surface is supposed to vary with the distance x from the slit.

The continuity, momentum, and thermal boundary layer equations are settled [15]:

$$\frac{\partial u}{\partial x} + \frac{\partial v}{\partial y} = 0 \tag{1}$$

$$\frac{\partial u}{\partial t} + u \frac{\partial u}{\partial x} + v \frac{\partial u}{\partial y} = \frac{\mu_{nf}}{\rho_{nf}} \frac{\partial^2 u}{\partial y^2} \tag{2}$$

$$\frac{\partial T}{\partial t} + u \frac{\partial T}{\partial x} + v \frac{\partial T}{\partial y} = \alpha_{nf} \frac{\partial^2 T}{\partial y^2} + \frac{\mu_{nf}}{(\rho C_p)_{nf}} \left(\frac{\partial u}{\partial y}\right)^2 \tag{3}$$

where u and v are the velocity component along x and y direction, respectively. The associated boundary condition is:

$$u = U_w, v = 0, T = T_w \text{ at } y = 0 \tag{4}$$

$$\frac{\partial u}{\partial y} = \frac{\partial T}{\partial y} = 0, v = \frac{dh}{dt} \text{ at } y = \delta, \tag{5}$$

where δ is the film thickness. The similarity transformation is defined as:

$$\eta = \left(\frac{b}{v(1-\gamma t)}\right)^{\frac{1}{2}} y, \psi(x, y, t) = \left(\frac{vb}{1-\gamma t}\right)^{\frac{1}{2}} x f(\eta), T(x, y, t) = T_0 - T_r \left(\frac{bx^2}{2v}\right) (1-\gamma t)^{-\frac{3}{2}} \theta(\eta) \tag{6}$$

The stream function $\psi(x, y)$ is defined as $u = \frac{\partial \psi}{\partial y}, v = -\frac{\partial \psi}{\partial x}$, where β is the dimensionless film thickness and is defined as,

$$\beta = \left(\frac{b}{v(1-\gamma t)}\right)^{\frac{1}{2}} h(t) \tag{7}$$

From Equation (7), we have:

$$\frac{dh}{dt} = -\frac{\gamma \beta}{2} \left(\frac{v}{b}\right)^{\frac{1}{2}} (1-\gamma t)^{-\frac{1}{2}} \tag{8}$$

Putting Equation (6) into Equations (2)–(4), and Equation (5), we obtain the following coupled system of ordinary differential equations.

$$f''' + (1-\phi)^{2.5} \left(1-\phi + \phi \frac{\rho_s}{\rho_f}\right) \left[f f'' - (f')^2 - \frac{S}{2} \left(f' + \frac{\eta}{2} f''\right) \right] - (1-\phi)^{2.5} f' = 0 \tag{9}$$

$$\frac{k_{nf}}{k_f} \theta'' + Pr \left[(1-\phi) + \phi \frac{(\rho C_p)_s}{(\rho C_p)_f} \right] \left[f \theta' - 2f' \theta - \frac{S}{2} (3\theta + \eta \theta') \right] + Ec (f'')^2 = 0 \tag{10}$$

Here the prime denotes the differentiation with respect to the similarity variable η and dimensionless parameters S , Pr , and Ec are unsteadiness parameters and defined as:

$$S = \frac{\gamma}{b'}, \quad Pr = \frac{v_{nf}}{\alpha_f}, \quad Ec = \frac{U_w^2}{C_p(T_w - T_0)} \tag{11}$$

The transform boundary conditions are,

$$f(0) = 0, \quad f'(0) = 1, \quad f(\beta) = \frac{S\beta}{2}, \quad f''(\beta) = 0, \quad \theta(0) = 1, \quad \theta'(\beta) = 0 \tag{12}$$

The physical quantities of interest are the skin friction coefficient C_{nf} , and the local Nusselt number Nu , which is defined as,

$$C_{nf} = \frac{\tau_w}{\frac{1}{2}\rho U_w^2}, \quad Nu = \frac{q_w}{k(T_w - T_0)}x \tag{13}$$

where $\tau_w = \mu\left(\frac{\partial u}{\partial y}\right)_y = 0$, $q_w = -k\left(\frac{\partial T}{\partial y}\right)_y = 0$ and $q_m = -D_B\left(\frac{\partial C}{\partial y}\right)_y = 0$, are the shear stress heat and mass fluxes at the surface, respectively, using the variables in Equation (7). The associated expressions for dimensionless skin friction coefficient C_{nf} reduced the Nusselt number $-\theta'(0)$ and reduced Sherwood number $-\phi'(0)$ are defined as,

$$Re_x^{\frac{1}{2}}C_p = -f''(0), \quad Re_x^{-\frac{1}{2}}Nu_x = -\theta'(0) \tag{14}$$

3. Method of Solution

Using the initial estimated values and auxiliary linear operators from Equations (9) and (10),

$$f_0(\eta) = \frac{3}{2\beta^2}(2 - S)\left[\frac{x^3}{6} - \frac{\beta x^2}{2}\right] + x, \quad \theta_0(\eta) = 1 \tag{15}$$

$$L_f = \frac{d^4 f}{d\eta^4}, \quad L_\theta = \frac{d^2 \theta}{d\eta^2}, \tag{16}$$

with constant properties:

$$L_f(C_1 + C_2\eta + C_3\eta^2 + C_4\eta^3) = 0 \quad \text{and} \quad L_\theta(C_5 + C_6\eta) = 0 \tag{17}$$

where C_i ($i = 1, 2, \dots, 6$) are arbitrary constants, which are included in general solution.

The average squared residuals error is presented so the Equations (10), (11) and (13) can be written as:

$$\epsilon_m^f = \frac{1}{n+1} \sum_{j=1}^n \left[\kappa_f \left(\sum_{j=1}^n f(\eta)_{\eta=j\delta\eta} \right) \right], \tag{18}$$

$$\epsilon_m^\theta = \frac{1}{n+1} \sum_{j=1}^n \left[\kappa_\theta \left(\sum_{j=1}^n f(\eta)_{\eta=j\delta\eta}, \sum_{j=1}^n \theta(\eta)_{\eta=j\delta\eta} \right) \right], \tag{19}$$

$$\epsilon_m^t = \epsilon_m^f + \epsilon_m^\theta \tag{20}$$

4. Table Discussion

Table 1 shows the numerical values of skin friction coefficient for different physical parameters. Here by increasing the value dimensionless film thickness parameter β and unsteady parameter S the values of skin friction also increase, if we increase the value of unsteady parameter S the skin friction coefficient value is increased.

Table 1. The numerical values for the skin friction coefficient for different physical parameters when $h = -0.1, Pr = 0.7, Ec = 0.1, \beta = 0.1$.

β	S	$f''(0)$	$f''(0)$	$f''(0)$	$f''(0)$
		GO-W $\phi=0.01$	GO-W $\phi=0.02$	GO-EG $\phi=0.01$	GO-EG $\phi=0.02$
0.1	0.1	30.3264	30.3335	28.7696	30.4545
0.2	-	30.3140	30.3412	30.3040	30.3414
-	0.2	30.2883	30.3261	30.2830	30.3264
-	0.3	30.7430	28.7777	28.1609	28.7778

Table 2 shows the numerical values of the local Nusselt number for various physical parameters. Here for increasing the values of Prandtl number Pr and unsteady parameter Eckert number Ec , the value of local Nusselt number Nu also increases.

Table 2. The numerical values of local Nusselt numbers of different physical parameters, when $\beta = 0.1, h = -0.1, S = 0.1$.

Ec	Pr	$\theta'(0)$	$\theta'(0)$	$\theta'(0)$	$\theta'(0)$
		GO-W $\phi=0.01$	GO-W $\phi=0.02$	GO-EG $\phi=0.01$	GO-EG $\phi=0.02$
0.1	0.5	-0.1437	-0.4409	-0.62116	-0.4411
0.2	-	-1.2456	-1.2571	-1.2458	-1.2576
0.3	-	-1.8697	-1.8869	-1.8700	-1.8875
-	0.6	0.6026	-1.8337	-0.6027	-0.6098
-	0.7	0.5870	-1.8875	-0.5871	-0.5952

Tables 3 and 4 represent the individual’s average square residuals error of Water-Graphene Oxide and Ethylene Glycol-Graphene Oxide executed for different order of approximation. We also noticed that the average square residual error value can be reduced by increasing the order of approximation where m represents the number of iterations.

Table 3. Individual averaged squared residual errors for graphene oxide water based nanofluid (GO-W) when $Pr = 6.5, Ec = 0.5, Nu = 0.1, S = 0.4, \beta = 0.3, \phi = 0.1$.

m	ϵ_m^f GO-W	ϵ_m^θ GO-W
6	1.7784×10^{-2}	1.91773×10^{-1}
12	9.14122×10^{-4}	8.77139×10^{-2}
18	6.97126×10^{-5}	5.4508×10^{-4}
24	6.44141×10^{-6}	3.79449×10^{-5}
30	6.50496×10^{-7}	2.7782×10^{-6}

Table 4. Individual averaged squared residual errors for graphene oxide ethylene glycol based nanofluid (GO-EG) when $Pr = 6.5, Ec = 0.5, Nu = 0.1, S = 0.4, \beta = 0.3, \phi = 0.1$.

m	ϵ_m^f GO-EG	ϵ_m^θ GO-EG
6	1.82761×10^{-2}	1.91773×10^{-1}
12	9.55814×10^{-4}	8.77139×10^{-2}
18	7.39644×10^{-5}	5.4508×10^{-4}
24	6.93791×10^{-6}	3.79449×10^{-5}
30	7.1187×10^{-7}	2.7782×10^{-6}

5. Result and Discussion

The geometry of the problem is displayed in Figure 1. Figures 2 and 3 indicate the sum of the square residual errors for the velocity pitch and temperature distribution up to the 30th order approximation. These figures show that the convergence of the obtained results is very strong for the proposed problem. These figures show that the increasing order of approximation enhances the convergence rate.

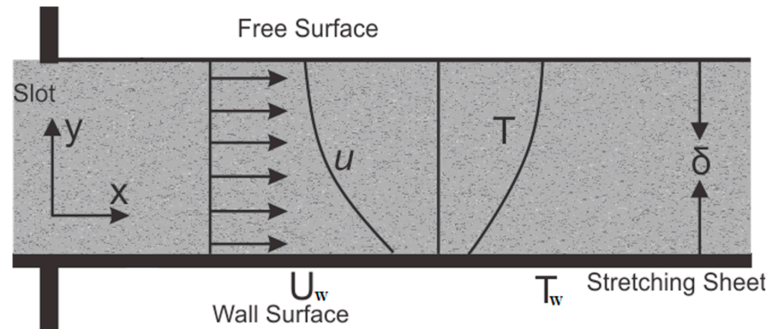


Figure 1. The physical sketch of the problem.

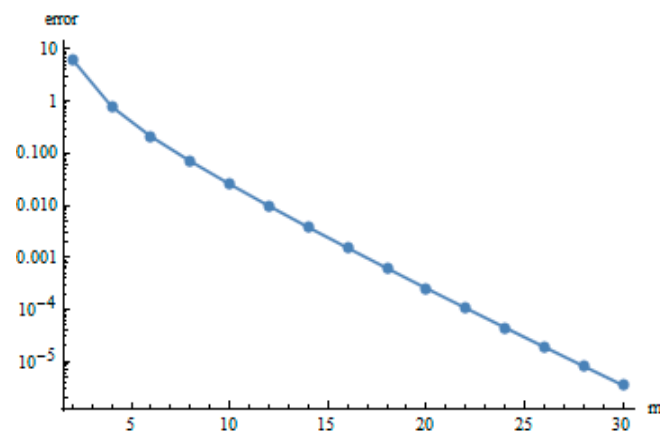


Figure 2. Individual average squared residual errors for EG-W.

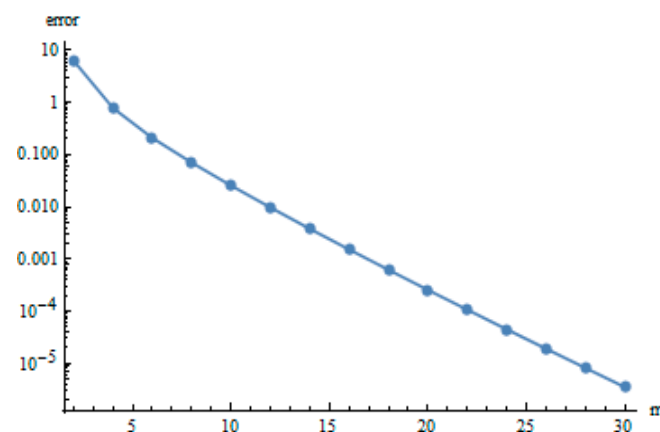


Figure 3. Individual averaged squared residual errors for GO-EG.

From Figure 4 we observe that if we increase the amount of the thin film thickness parameter β , there is an effect on the velocity profile due to increasing β , meaning that the resistance force increases and consequently the velocity profile decays. In fact, the increasing thickness improves the resistance force and the fluid motion is retarded. The decay effect is comparatively larger in the GO-EG. From

Figure 5 we observe that increasing values of the nanoparticle volume fraction ϕ raises the velocity near the sheet surface and the velocity field is delayed after the point of inflection. This effect is comparatively strong in the GO-EG. In fact, the thermophysical properties of the EG is comparatively larger than the water and consequently the increasing value of the nanoparticle volume fraction increases the velocity field.

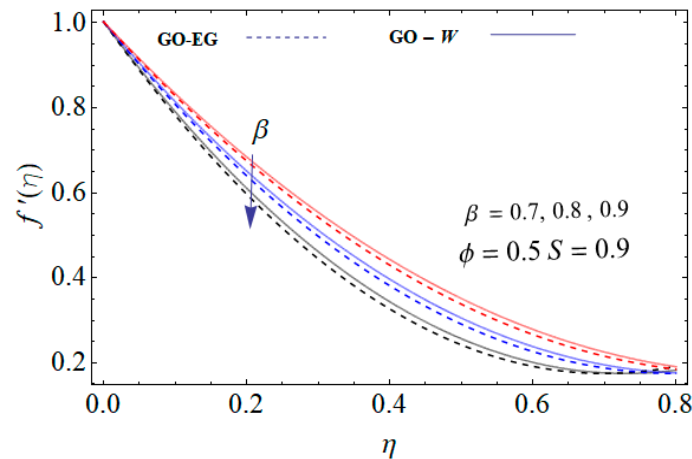


Figure 4. Effect of the dimensionless film thickness parameter β versus velocity profile.

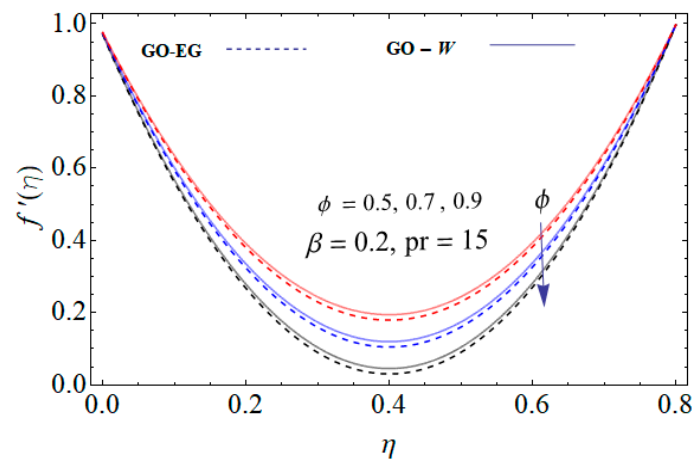


Figure 5. Effect of dimensional less nanoparticle volume fraction ϕ on velocity profile.

Figure 6 shows the effect of the unsteadiness parameter S on the velocity profile. The dimensional axial velocity decreases with increases in the unsteadiness parameter S . Actually, the increasing value of S increases the thickness of the momentum boundary layer and consequently the velocity field reduces. This impact is identical for both sorts of nanofluids. Figure 7 indicates the increase in the Prandtl number, thus decreasing the temperature profile. In fact, when the thickness of the momentum boundary layer is larger than that of the thermal boundary layer, or the viscous diffusion is larger than the thermal diffusion, the larger amount of the Prandtl number reduces the thermal boundary layer.

Figure 8 indicates that increasing values of the nanoparticle volume fraction raises temperature. This effect is comparatively strong in the GO-W. In fact, the increasing value of the nanoparticle volume fraction enhances the thermal efficiency of the nanofluid and consequently the temperature field increases. From Figure 9, the relation between the Eckert number and temperature profile is a direct relationship to the physical study of this result, by increasing the Eckert number it will enhance the kinetic energy due to the intermolecular collision and consequently the temperature profile increases. In fact, the viscous dissipation is the key agent in this whole phenomenon and as a result the larger value of the Eckert number enhances the temperature field.

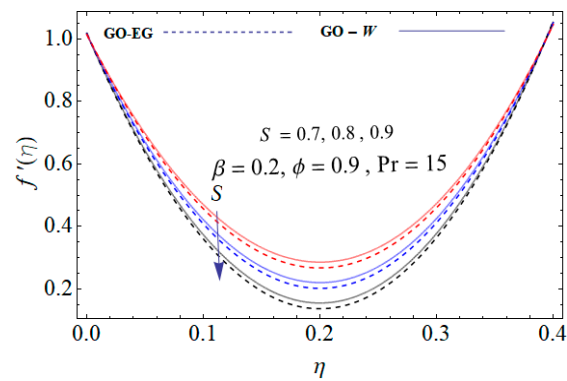


Figure 6. Effect of the unsteadiness parameter on the velocity profile.

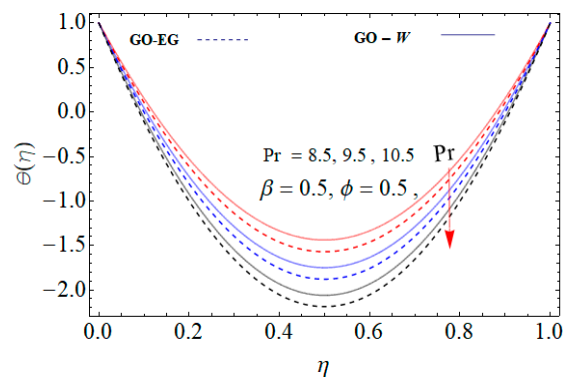


Figure 7. Effect of Prandtl number versus temperature profile.

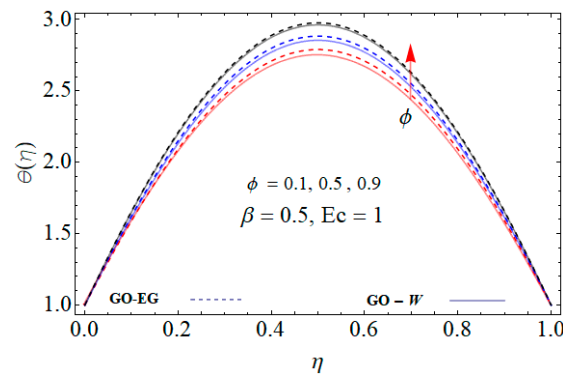


Figure 8. Effect of dimensionless nanoparticle volume fraction on temperature profile.

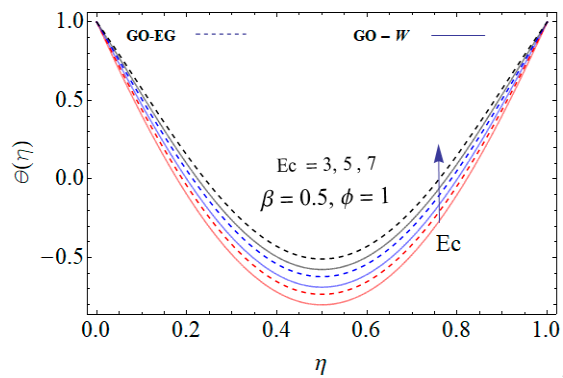


Figure 9. Effect of Eckert number on the temperature profile.

6. Conclusions

The thin film of nanofluids over an unstable and flexible sheet has been considered. The GO-W and GO-EG nanofluids have been compared for the heat transfer enhancement applications. The GO-EG nanofluid has stronger thermal conductivity and; therefore, it is concluded that the GO-EG nanofluid is more efficient for the heat transfer enhancement as compared to the GO-W nanofluid. The OHAM technique has been used for the solution of the problem and the strong convergence has been achieved through the residual analysis. The impact of the physical constraints versus the velocity and temperature profiles have been plotted and discussed. The main points are pointed out as:

- By increasing the unsteadiness parameter S the velocity profile decreases and this effect is comparatively strong in the GO-EG nanofluid.
- The increasing value of the Prandtl number reduces the temperature profile. The effect is comparatively strong using the GO-EG nanofluid.
- Increasing the Eckert number increases the kinetic energy to enhance the temperature field.
- The increasing thickness of the thin film reduces the fluid motion.

Author Contributions: Conceptualization, A.R. and T.G.; methodology, T.G.; software, A.R.; validation, A.R. and T.G.; formal analysis, Z.Z.; writing—original draft preparation, T.G. & A.R.; writing—review and editing, Z.Z. & Z.S.; supervision, Z.S. and T.G.; project administration, Z.S.; funding acquisition, Z.S.

Funding: This research received no external funding.

Conflicts of Interest: The authors declare no conflict of interest.

Nomenclatures

g	Acceleration due to gravity (ms^{-2})
μ_{nf}	Dynamic viscosity of the nanofluids axial directions (kgms^{-1})
ρ_{nf}	Density of the nanofluids (kgm^{-3})
Ec	Eckert number ($\frac{\mu c_p}{k_0}$)
Q	Heat generation/absorption parameter (deg)
T	Local temperature (K)
β	Non-dimensional thickness of the liquid film
Nu	Nusselt number ($rq_w \theta = \alpha \backslash k_0 T_w$)
Pr	Prandtl number ($\frac{U^2}{C_p T_w}$)
C_p	Specific heat ($\text{Jkg}^{-1}\text{K}^{-1}$)
W_w	Stretching velocity (ms^{-1})
η	Similarity variable ($\frac{\theta}{\alpha}$)
C_f	Skin friction ($\frac{\tau_w}{\rho U^2}$)
φ	Solid particle volume fraction
δ	Thickness of the liquid film
T_δ	Temperature at the free surface (K)
k_{nf}	Thermal conductivity of the nanoparticles ($\text{WM}^{-1}\text{K}^{-1}$)
(u, w)	Velocity components (ms^{-1})

References

1. Choi, S.U.S.; Estman, J.A. Enhancing thermal conductivity of fluids with nanoparticles. *ASME Publ. Fed* **1995**, *231*, 99–106.
2. Choi, S.U.; Zhang, Z.G.; Yu, W.; Lockwood, F.E.; Grulke, E.A. Anomalous thermal conductivity enhancement in nanotube suspensions. *Appl. Phys. Lett.* **2001**, *79*, 2252. [[CrossRef](#)]
3. Haq, R.U.; Kazmi, S.N.; Mekkaoui, T. Thermal management of water based SWCNTs enclosed in a partially heated trapezoidal cavity via FEM. *Int. J. Heat Mass Transf.* **2017**, *112*, 972–982. [[CrossRef](#)]

4. Soomro, F.A.; Haq, R.U.; Khan, Z.H.; Zhang, Q. Passive control of nanoparticle due to convective heat transfer of Prandtl fluid model at the stretching surface. *Chin. J. Phys.* **2017**, *55*, 1561–1568. [[CrossRef](#)]
5. Yu, W.; Xie, H.Q.; Chen, L.F.; Li, Y. Investigation on the thermal transport properties of ethylene glycol-based nanofluids containing copper nanoparticles. *Powder Technol.* **2010**, *197*, 218–221. [[CrossRef](#)]
6. Xie, H.Q.; Chen, L.F.J. Review on the preparation and thermal performances of carbon nanotube contained nanofluids. *Chem. Eng. Data* **2011**, *56*, 1030–1041. [[CrossRef](#)]
7. Xiao, B.; Yang, Y.; Chen, L. Developing a novel form of thermal conductivity of nanofluids with Brownian motion effect by means of fractal geometry. *Powder Technol.* **2013**, *239*, 409–414. [[CrossRef](#)]
8. Buongiorno, J. Convective transport in nanofluids. *ASME J. Heat Transf.* **2006**, *128*, 240–250. [[CrossRef](#)]
9. Khan, W.A.; Pop, I. Boundary layer flow of a nanofluid past a stretching sheet. *Int. J. Heat Mass Transf.* **2010**, *53*, 2477–2483. [[CrossRef](#)]
10. Shah, Z.; Gul, T.; Khan, M.A.; Ali, I.; Islam, S.; Hussain, F. Effects of hall current on steady three dimensional non-Newtonian nanofluid in a rotating frame with Brownian motion and thermophoresis effects. *J. Eng. Technol.* **2017**, *6*, 280–296.
11. Balandin, A.A.; Ghosh, S.; Bao, W. Superior thermal conductivity of single-layer graphene. *Nano Lett.* **2008**, *8*, 902–907. [[CrossRef](#)] [[PubMed](#)]
12. Wei, Y.; Huaqing, X.; Dan, B. Enhanced thermal conductivities of nanofluids containing graphene oxide nanosheets. *Nanotechnology* **2010**, *21*, 055705.
13. Gul, T.; Firdous, K. The experimental study to examine the stable dispersion of the graphene nanoparticles and to look at the GO-H₂O nanofluid flow between two rotating disks. *Appl. Nanosci.* **2018**, *8*, 1711–1727. [[CrossRef](#)]
14. Gul, T.; Noman, W.; Sohail, M.; Khan, M.A. Impact of the Marangoni and thermal radiation convection on the graphene-oxide-water-based and ethylene-glycol-based nanofluids. *Adv. Mech. Eng.* **2019**, *11*, 1–9. [[CrossRef](#)]
15. Qasim, M.; Khan, Z.H.; Lopez, R.J.; Khan, W.A. Heat and mass transfer in nanofluid thin film over an unsteady stretching sheet using Buongiorno's model. *Eur. Phys. J. Plus* **2016**, *131*, 16. [[CrossRef](#)]
16. Alshomrani, A.S.; Gul, T. The convective study of the Al₂O₃-H₂O and Cu-H₂O nano-liquid film sprayed over a stretching cylinder with viscous dissipation. *Eur. Phys. J. Plus* **2017**, *132*, 495. [[CrossRef](#)]
17. Gul, T.; Nasir, S.; Islam, S.; Shah, Z.; Khan, M.A. Effective Prandtl number model influences on the γ Al₂O₃-C₂H₆O₂ and γ Al₂O₃-H₂O nanofluids spray along a stretching cylinder. *Arab. J. Sci. Eng.* **2018**, *44*, 1601–1616. [[CrossRef](#)]
18. Aziz, R.C.; Hashim, I.; Alomari, A.K. Thin film flow and heat transfer on an unsteady stretching sheet with internal heating. *Meccanica* **2011**, *46*, 349–357. [[CrossRef](#)]
19. Pour, M.S.; Nassab, S.G. Numerical investigation of forced laminar convection flow of nanofluids over a backward facing step under bleeding condition. *J. Mech.* **2012**, *28*, 7–12. [[CrossRef](#)]
20. Abu-Nada, E. Numerical prediction of entropy generation in separated flows. *Entropy* **2005**, *7*, 234–252. [[CrossRef](#)]
21. Abu-Nada, E. Application of nanofluids for heat transfer enhancement of separated flows encountered in a backward facing step. *Int. J. Heat Fluid Flow* **2008**, *29*, 242–249. [[CrossRef](#)]
22. Liao, S.J. The Proposed Homotopy Analysis Method for the Solution of Nonlinear Problems. Ph.D. Thesis, Shanghai Jiao Tong University, Shanghai, China, June 1992.
23. Liao, S.J. *Advances in the Homotopy Analysis Method*; World Scientific Press: Singapore, 2013.
24. Rehman, A.; Gul, T.; Salleh, Z.; Mukhtar, S.; Hussain, F.; Nisar, K.S.; Kumam, P. Effect of the Marangoni convection in the unsteady thin film spray of CNT nanofluids. *Processes* **2019**, *7*, 392. [[CrossRef](#)]
25. Gul, T.; Sohail, M. Marangoni liquid film scattering over an extending cylinder. *Theor. Appl. Mech. Lett.* **2019**, *9*, 106–112. [[CrossRef](#)]
26. Khan, N.S.; Gul, T.; Kumam, P. Influence of inclined magnetic field on Carreau nanoliquid thin film flow and heat transfer with graphene nanoparticles. *Energies* **2019**, *12*, 1459. [[CrossRef](#)]
27. Ali, V.; Gul, T.; Afridi, S.; Ali, F.; Alharbi, S.O.; Khan, I. Thin film flow of micropolar fluid in a permeable medium. *Coatings* **2019**, *9*, 98. [[CrossRef](#)]
28. Gul, T.; Khan, W.A.; Tahir, M.; Bilal, R.; Khan, I.; Nisar, K.S. Unsteady Nano-Liquid spray with thermal radiation comprising CNTs. *Processes* **2019**, *7*, 181. [[CrossRef](#)]

29. Gul, T.; Khan, A.S.; Islam, S. Heat transfer investigation of the unsteady thin film flow of Williamson fluid past an inclined and oscillating moving plate. *Appl. Sci.* **2017**, *7*, 369. [[CrossRef](#)]
30. Khan, W.; Gul, T.; Idrees, M.; Islam, S.; Khan, I.; Dennis, L.C.C. Thin film Williamson nanofluid flow with varying viscosity and thermal conductivity on a time-dependent stretching sheet. *Appl. Sci.* **2016**, *6*, 334. [[CrossRef](#)]



© 2019 by the authors. Licensee MDPI, Basel, Switzerland. This article is an open access article distributed under the terms and conditions of the Creative Commons Attribution (CC BY) license (<http://creativecommons.org/licenses/by/4.0/>).